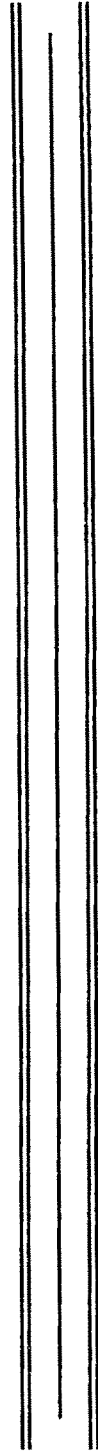


CHAPTER - 5
FERRICRETES



FERRICRETES

INTRODUCTION

Ever since Buchanan (1807) introduced the term **Laterite** - *a rock full of cavities and pores that contains a very large quantity of iron in the form of red and yellow ochers*, and the subsequent studies through multi disciplinary approach have resulted into voluminous literature pertaining to its chemistry, mineralogy, petrography, genesis (Mc Farlane, 1971; Mc Farlane, 1976, 1983a, 1983b; Valetton, 1983; Nahon,1977,1983). Also, its applications in geotechnical, palaeoclimatic and economic geological aspects (Giddigasu, 1983, 1987; Nair et al., 1987; Esson, 1983) have made laterites an important litho-stratigraphic unit.

Inspite of wealth of information now available on the laterites, the controversies still persists on the exact definition of laterites. This has resulted in the origin of various terminologies viz. iron hat, ferricretes, fersilitic, fersialitic and ferralitic soils for laterites and akin deposits.

Schellman (1981) after a thorough review of the nomenclatures, suggested the following definition for laterites.

"Laterites are the products of intense sub-aerial rock weathering whose iron and or alumina content is higher and silica content is lower than in merely kaolinized parent

rocks. They consist predominantly the mineral assemblages viz. goethite, hematite, hydroxides of alumina, kaolin and quartz ".

Lamplugh (1907) almost a century ago coined the term **Ferricrete** to describe iron rich crusts consisting largely of nodular to massive or vesicular oxides and hydroxides of iron with or without kaolin and lithic fragments (Ollier, 1984).

Woolnough's (1927) terminology duricrust though embrace these insitu, residual sesquioxides rich deposits, Lamplugh's (1907) ferricrete has been preferred by the author in concurrence with Nahon (1987) to describe the reddish, hard, indurated, iron rich deposits observed in the study area, on account of their ubiquitous prevalence as cappings, over a poorly preserved weathering profile.

DISTRIBUTION OF FERRICRETES

Within the study area ferricretes confine to narrow strip in the Jaisalmer basin, from Bersi in the southern part to Mohangarh in the northeast (Figure 4.1) and occur as cappings over the mesa's, buttes and highlevel rocky plains. However, their occurrence at lower levels (around Habur, Ramgarh, Savanta) with a thin veneer of ferricretic lags are also evidenced. The development of ferricretes in the investigated area associate with different lithologies from Lathi sandstone (Jurassic age) to the sandstones and limestones (Sanu, Habur Formations) of Tertiary age. However, they are prominent and well developed with in the weathering profiles of Tertiaries.

In general, ferricretes of the study area show poor gradational contacts with the parent rock through a mottled, pallid zones. But, in some low level areas (around Habur) ferricretes occur immediately above the ferruginous sandstones, as completely dismantled relic's with yellowish brown limonitic materials at the top. In the study area, hard ferricretes are seen capping the relatively soft sandstones, resulting in the development of steeper slopes. They also show solution activities resulting in the formation of cavities and yellowish brown iron oxides. Recrystallization of silica, along the fractures and its coating

around the desiccated clayey surface is commonly observed in the mottled zone of the ferricrete profiles

The most salient feature of the ferricrete profiles of the investigated area is the dismantling of the ferricretes (up to the mottled horizon) and subsequent calcretization. The calcretization is evidenced to start as fracture fillings within the brecciated ferricretes. With the increase in intensity of calcretization, the calcretes bind the dismantled ferricrete breccias and develop a calcretic layer in between the mottled zone and the ferricrete proper. Formation of pseudomorphs of kaolin by calcite is also observed in the mottled horizons.

A typical ferricrete profile of the study area comprise the following sequence from top to bottom :

Ferricrete - calcretized
Mottled zone
Pallid zone
Bedrock.

CLASSIFICATION OF FERRICRETES

These residually formed iron cappings are classified on the basis of geological, pedological and geochemical aspects. The earliest classification of laterites has been attempted on the basis of $\text{SiO}_2 / \text{Fe}_2\text{O}_3$ ratio (Mortyn and Doyné, 1927). On the basis of this ratio the laterites were grouped into three categories viz. non-laterite soils ($\text{SiO}_2 / \text{Fe}_2\text{O}_3 > 2$); laterite soils ($\text{SiO}_2 / \text{Fe}_2\text{O}_3 = 1.33 - 2$) and laterite ($\text{SiO}_2 / \text{Fe}_2\text{O}_3 < 1.33$). Subsequently, Loachin and Kandiah (1941); Benjamin and Sktaley (1970) instead of $\text{SiO}_2 / \text{Fe}_2\text{O}_3$ ratio, used the molar ratios of silica to the sesquioxides (Fe_2O_3 and Al_2O_3) to arrive at the above classification.

Besides the chemical aspects, the ferricretes have also been classified on the following basis

- 1 Geomorphic association they are classified as highlevel and low level laterites (Mc Farlane, 1976).
- 2 Pedogenic laterites and groundwater laterites (Leprun, 1981) Further grouping of both ground-water and pedogenic laterites into immature (spaced pisolithic, packed pisolithic) mature varieties (massive vermiforms / cellular) was suggested by Mc Farlane (1976)
- 3 Primary laterites and secondary laterites on the basis of whether developed as insitu or reworked (Sahasrabudhe and Deshmukh, 1981)
4. On the basis of forms, Mc Farlane (1983a) grouped laterites into nodular, concretionary, pisolithic, and vermiform laterites.

Schellmann (1981) has classified the process of ferricretization into kaolinisation, weak lateritization, moderate lateritization and strong lateritization by considering the intensity of weathering, which is measured by the residual silica content in the ferricretes.

Taking into account the intricacies of different classifications, the author has preferred to adopt the classification of Mc Farlane (1983) due to its simplicity and easier field applicability. However, in order to have better understanding, the Schellmann's (1981) classification based on the chemistry is also incorporated under the present study

The ferricretes of the study area vary from the massive sheeted type (occurring around Chetral, Kaladongar areas) to pisolithic type (as seen in Savanta, RD 105, Ramgarh). In the study area, the upper part of the ferricrete profiles are ubiquitously dismantled, resulting in the formation of brecciated ferricretes. The pisolithic ferricretes observed in these profiles can further be divided into two categories viz

- 1 **Spaced pisolithic** - ferricretes are embedded in kaolinitic or siliceous matrix, which upon exposure forms released pisoliths on the surface.
- 2 **Packed pisolithic** ferricretes have the pisoliths well cemented in ferruginous material and are compact and massive in nature.

The brecciated ferricretes occupy as lags over the pisolithic ferricretes or along the piedmont slopes and pedimentary surfaces which intern have been subjected to calcretization during latter phases.

FIELD STUDIES

As it has already been elucidated earlier that ferricretes are confined to a narrow strip, dismantled and calcretized; occurrence of a typical ferricrete profile is seldom observed. However, the author in this present study has attempted to understand the genesis of calcretized ferricretes by way of studying their chemistry, mineralogy & micromorphology by making an inventory of profiles around the locations viz. RD 105, Ramgarh, Asutar, Khinya, Bandah, Chetral, Habur, Savanta, and Kaladongar.

PROFILE CHARACTERISTICS

RD 105 (N 27° 20' ; E 70° 45')

This profile forms a part of low level plateau surface adjacent to the Indira Gandhi canal near Sultana village. Here the ferricrete's capping is massive (about 2 - 2.5 m thick) and is of packed pisolithic type (Figure and Plate 5.1 [A]) in its upper part. This is followed by a formation of spaced pisolithic type of ferricretes (at depth 2.5 - 4.8 m). This can be attribute to the increase in siliceous and kaolin matrix with depth.

The mottled horizon lying below the spaced pisolithic zone includes kaolin and secondary silica, which in turn give way to the unmottled pallid horizon (depth > 5 m). Here, the bedrock is not traceable.

Ramgarh (N 27° 22' ; E 70° 32')

The 3.2 m thick ferricrete profile within a rocky undulating plain comprise upper 1.5 m thick calcretized ferricretes (Figure and Plate 5.1 [B]), followed by a 25 - 40 cm thick massive packed pisolithic ferricrete. The mottled horizon comprise a few spaced pisoliths within a kaolin-silica matrix and also have secondary silica. The mottled zone merges with a sharp boundary into the underlying nummulitic limestone.

Bandah (N 27° 10' ; E 70° 45')

This 4 m thick ferricrete profile comprise the upper most horizon of calcretized ferricretes, forming as a capping over mesas. Unlike the Ramgarh and RD 105 profiles, here the calcretization is intense. This has resulted into the reduction of the packed pisolithic horizon to about 10 to 15 cm thick (Figure 5.1 [C]; Plates 5.2 [A & B]). The Packed pisolithic ferricrete is followed by the spaced pisolithic variety and then the mottled zone. A thin calcrete layer encompassing the ferricrete pisoliths is also observed in between the mottled horizon and ferricrete proper. Here, the parent rock exposed at a depth of 3 m is a ferruginous sandstone.

Khinya (N 27° 20' ; E 70° 53')

Here, the plateau surfaces are capped by calcretized ferricretes of about 2.2 m thick. The fragmented ferricretes show different stages of calcretization from simple fracture filling to well developed calcretes encompassing ferricretic pisoliths and nodules (Figure 5.1 [D]; Plate 5.3 [A]). Oxidation of ferricretes, formation of solution cavities and leaching of yellowish brown iron oxides are also widely observed in the upper parts of the profile. Underlying unit is a well laminated clay free from any mottling and other features similar to that a lateritic profile. The basal horizon is a nummulitic limestone. All the three lithounits display sharp boundary conditions.

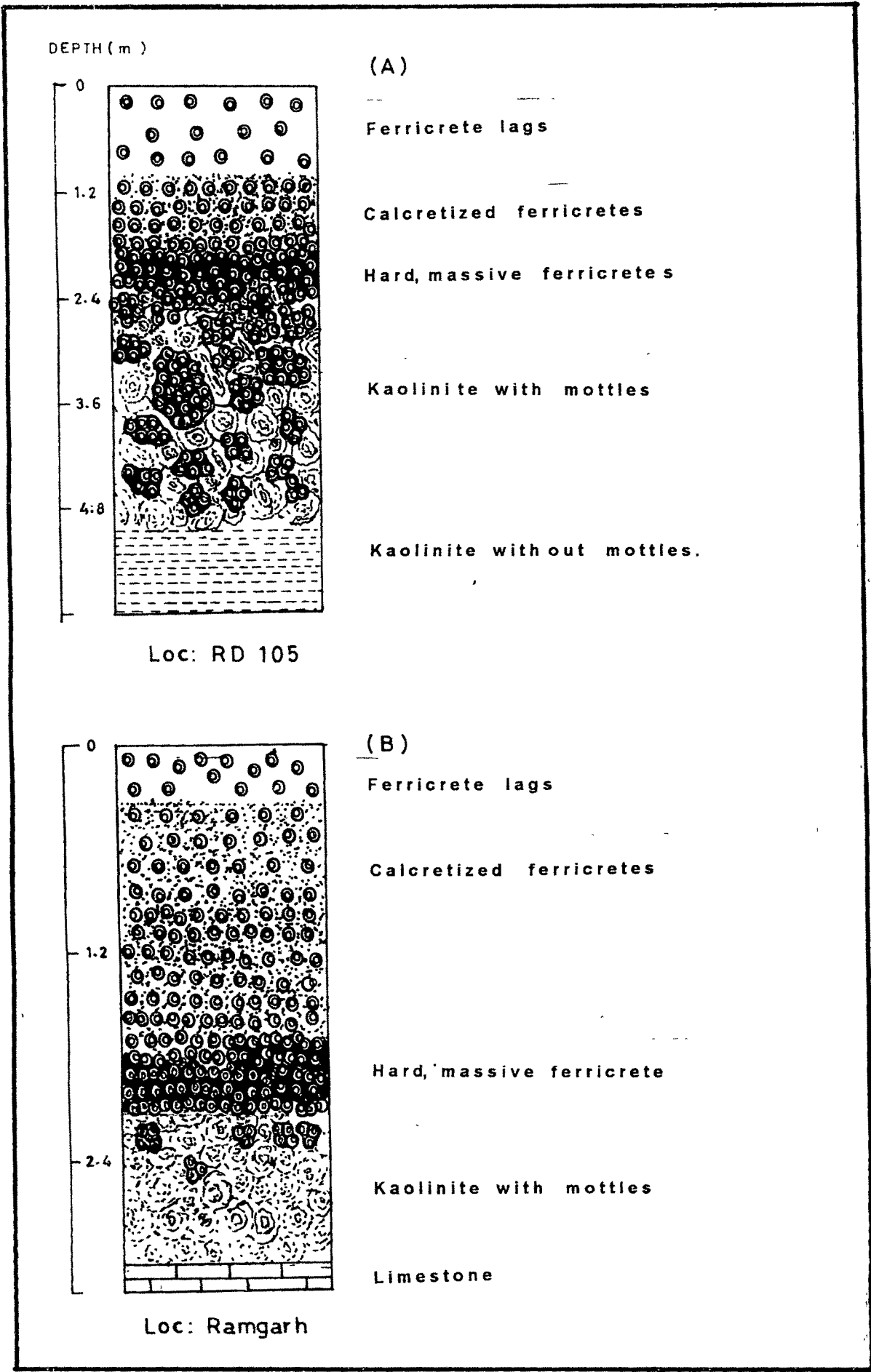


Fig. 5.1 Ferricrete profiles of the study area

Plate 5 1

- (A) A view of the massive ferricrete surface developed over Tertiary sandstones Loc RD 105 Indira Gandhi Canal, near Sultana
- (B) A dismantled calcretized ferricrete profile Loc Ramgarh



A

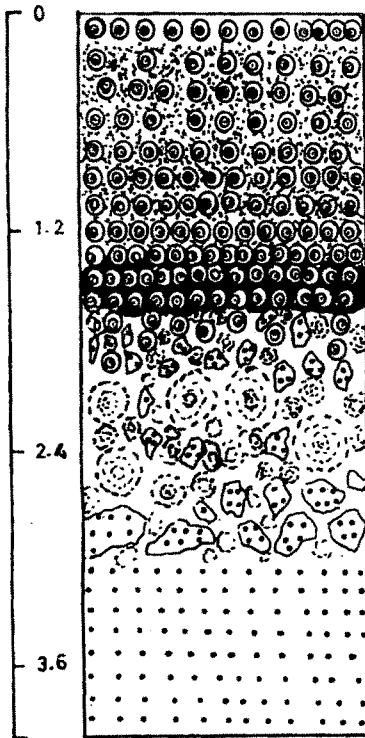


B

Plate 5.1

DEPTH (m)

(C)



Calcretized ferricrete

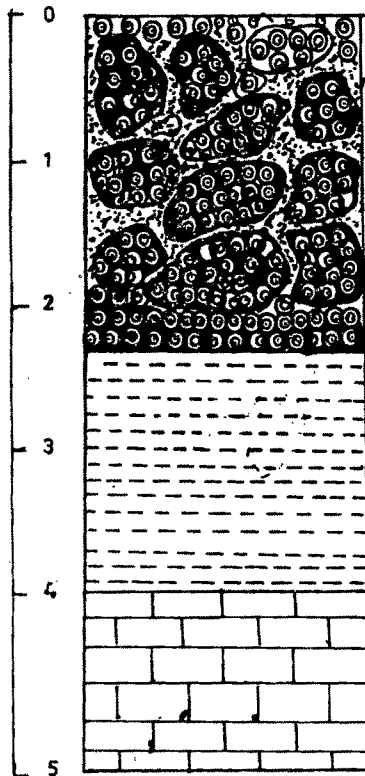
Ferricrete-packed pisolithic

Kaolinite with mottles

Sandstone

Loc: Bandah

(D)



Calcretized ferricrete

Laminated clay

Limestone

Loc: Knenya

Fig. 5.1 Ferricrete profiles of the study area

Plate 5.2

- (A) Calcretized - ferricrete capping over isolated plateauic surfaces. Loc. Nr. Bandah.
- (B) A close view of above duricrust depicting fragments of calcretized ferricretes.



A



B

Plate 5.2

Similar ferricrete profiles are also seen over nummulitic limestones near **Asutar** (near Shahgarh). These ferricretic duricrusts, which constitute a part of rocky plains consists of upper calcretized ferricretes (brecciated) - packed pisolithic ferricrete - mottled kaolin horizons (Figure 5.1 [E]).

Savanta (N 26° 40' ; E 71° 20')

A 3 m thick ferricrete profile developed on Lathi sandstones (Jurassic). This profile comprise upper massive ferricrete sheets with occasional pisoliths. Development of iron hydroxides and caverns are significant features of this horizon (Figure 5.1 [F]; Plate 5.3 [B]).

Sheeted type of ferricretes progressively grade downward into a horizon of packed pisolithic ferricretes of 1 m thickness. The Packed pisolithic ferricrete gradually merges with the underlying spaced pisolithic variety which is followed by horizon of Kaolinite.

Kaladongar (N 71° 15' ; E 27° 20')

Ferricretic duricrusts of sheeted nature forms a capping over the series of isolated hills. The total thickness of the profile is about 10 m and is developed over fine grained sandstone (Plate 5.4 [A]). The Ferricretes show intense solution activities and is highly cavernous (Plates 5.4 [B]. Here, the development of sheet type of ferricretes from the pisolithic varieties are evidenced by way of intense ferruginous cementing. The calcretization is very weak and is occasionally seen as tubules along the fractures. The mottled zone is about 1 m thick, comprising iron mottles within kaolin.

Chetral (N 26° 58' ; E 70° 42')

Akin to the Kaladongar, the sheeted ferricretes here too form capping over isolated hills and plateaus (Figure 5.1 H, Plate 5.5 A). However, unlike the Kaladongar, calcretes here are well developed along the fractures and planar voids giving a paradoxical appearance of alternate layering of ferricretes and calcretes. The packed pisolithic ferricrete is about

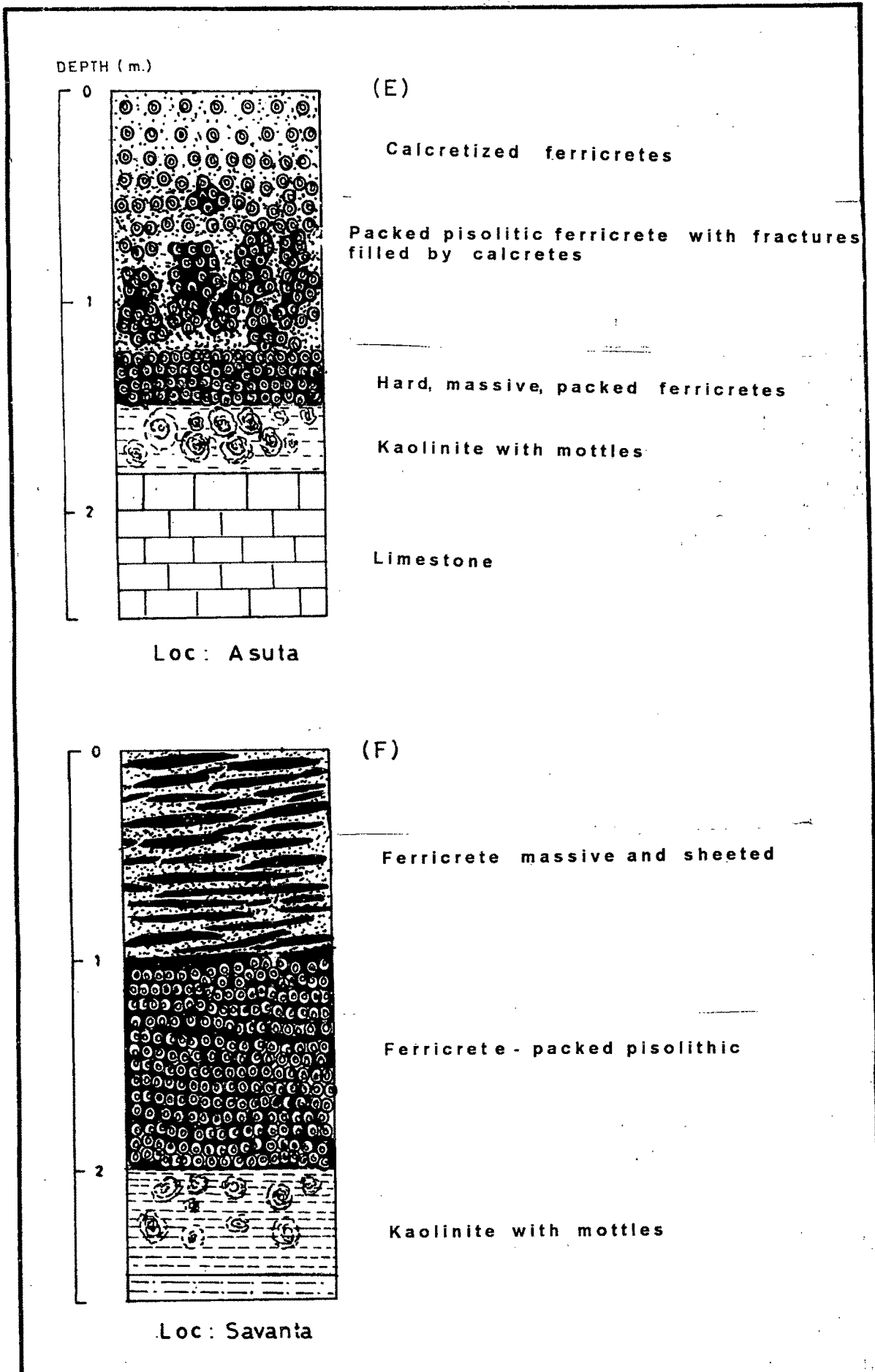


Fig. 5.1. Ferricrete profiles of the study area

Plate 5.3

- (A) Calcretized ferricretes as capping over Plateaus. Loc. Khenya.
- (B) Sheet type ferricretes developed over Lathi sandstone (Jurassic). Loc. Savanta.



A



B

Plate 5.3

Plate 5.4

- (A) A view of ferricrete profile developed over sandstone.
Loc. Kaladongar.
- (B) A close view of above ferricrete surface showing dissolution features.



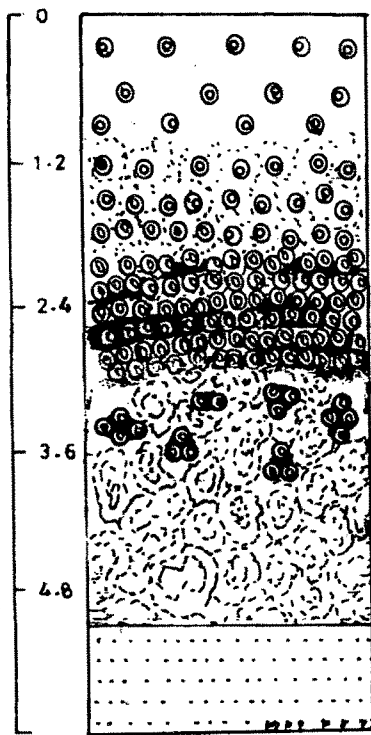
A



B

Plate 5.4

DEPTH (m)



(G)

Ferricrete lags

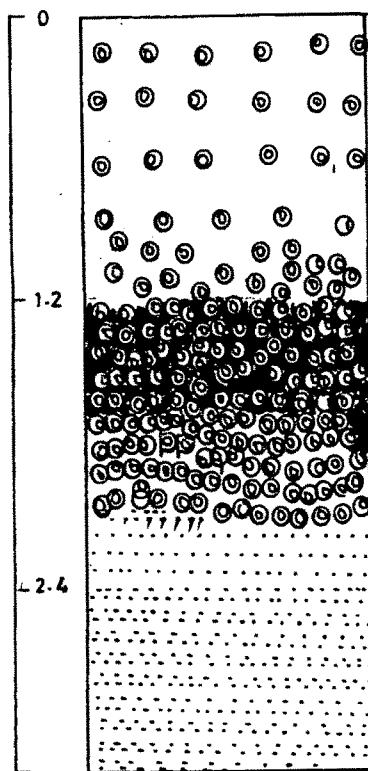
Ferricrete-calcretized

Packed pisolitic ferricrete

Kaolinite with mottles

Ferruginous sandstone

Loc: Chetral



(H)

Ferricrete lags

Ferricrete-brecciated

Ferruginous sandstone

Loc: Habur

Fig. 5:1 Ferricrete profiles of the study area

Plate 5.5

- (A) Multi layered ferricrete sheets forming a cap over Tertiary sandstone. Loc. Chetral.
- (B) A view of ferricrete pedimentary surface. Loc. Near Khuyala.



A



B

Plate 5.5

0.40 m thick and is followed by kaolinite horizon having mottles in its upper part. The parent rock is ferruginous sandstone.

Habur (N 27° 10' ; E 70° 35')

A totally dismantled ferricrete profile with relics of iron pisoliths and caverny, oxidized ferricretic fragments are observed resting directly over the ferruginous sandstone. Subsequent recementation by iron oxides resulted in the formation of spaced pisolithic kind of ferricretes at a depth of 1.2 - 1.5 m. However, the underlying loose brecciated ferricretes indicate that the recementing is a latter phenomena after the dismantling of the ferricrete profile. Similar brecciated ferricretes are widely observed as a pediment surfaces around Khiyala (Plate 5.5 B).

MICROMORPHOLOGY OF FERRICRETES

On account of the opaque nature of the ferricretes, the pedogenic sequence of ferricretization couldn't be completely understood, using micromorphological techniques. However, the stages of ferricretization can be interpreted from the mineral assemblages, stages of mineral weathering and neoformations. The subsequent phase of dismantling of ferricrete profiles, different phases of calcretization, ongoing process of ferricrete replacement by calcretes are very well documented and can be recognized under the microscope. Thus, for understanding the processes of ferricretization and the latter changes within the profile micromorphological techniques play a key role. Some of the important micromorphic features identified and their implications are discussed here under:

Sheeted and packed ferricretes often show vesicles and channels either unfilled (Plate 5.6 [A]) or filled with the yellowish brown ironoxides. Occasionally they also incorporate fibrous clayey materials. These features strongly suggests the role of pedogenesis in ferricrete formation (Mc Farlane, 1976; Bullock et al. 1985)

The ferricretes comprise exclusively quartz detritals with in an opaque to translucent ferruginous cement. These quartz detritals are strongly etched, corroded and dissolved (Plate 5.6 [B]) Such characteristics point to extreme stage of ferricretization, where in quartz detritals are dissolved (desilicification) in an acidic environment with the aid of sesquioxides

Kaolinized, etched, dissolved feldspars in the mottled horizon (Plate 5 6 [C]) without any relic textural features of the parent rock point to the progradational stages of conventional lateritic profiles, which ultimately lead to the development of ferricretes Big nodules of iron encompassing the yellowish brown clayey matter is also characteristic features in this horizon.

However, the pallid horizons have both relics textural features of parent rock and the altered feldspar detritals within a clayey plasma. Iron segregation is evidenced as small opaque to translucent nodules and mottles (Plate 5.6 [D]).

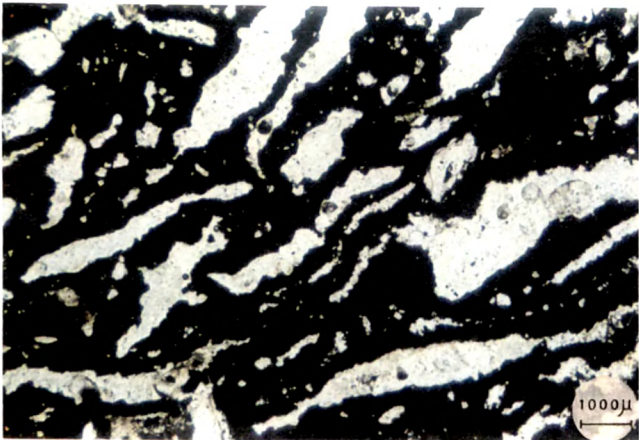
The dismantling of ferricretes results into solution activity along different layers of pisoliths there by, forming alternate layers of opaques and translucent yellowish brown iron oxides (Plate.5.6 [E]). Progression of solution results in the peeling of individual layers and destruction of the pisoliths to form cavities (Bullock et al,1985).

The first phase of calcretization is evidenced by the clear, very coarse sparitic crystals, filling the vesicles (Plate 5.6 [F]), cavities (Plate 5.7 [A]), fractures and as pendent cements (Plate 5.7 [B]). Replacement of the detritals and ferruginous cement by the sparites is also evidenced in fractures (Plate 5.7 [C & D]). The channels are filled by sparites without any iron stain. But, iron stained and fine laminations are seen along the channel walls. This feature can be attributed to replacement of ferruginous cement by calcite or alternate coating of ferruginous cement and calcite.

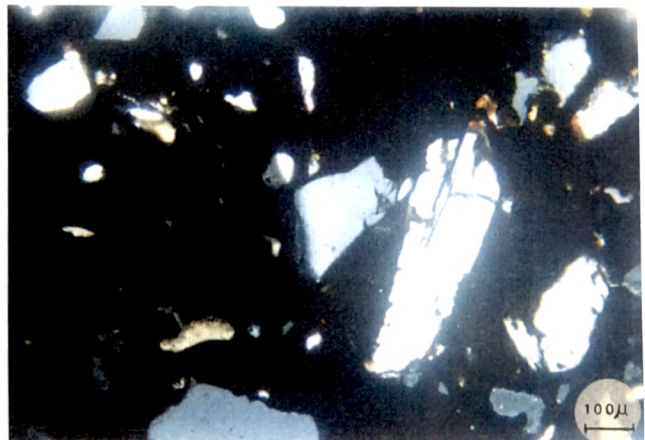
Presence of secondary silica within the channels is ubiquitously observed in the upper part of the mottled zone in almost all the profiles studied. Their occurrence with the calcite is seldom observed (Plate 5.7 [E]). The presence of secondary silica could be attributed to

Plate 5.6 Photomicrographs of ferricrete profiles illustrating

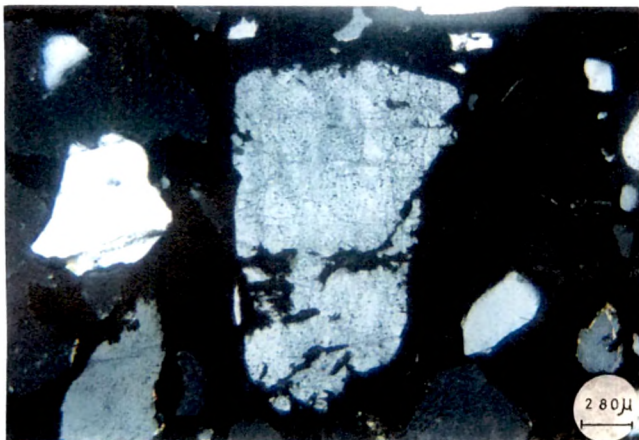
- (A) Vesicular structure suggestive of pedogenic activity.
- (B) Desilicification features in ferricretes, indicative of lateritic weathering.
- (C) Kaolinised, corroded, dissolved feldspar in mottled horizon a characteristic feature of lateritic weathering.
- (D) Relics of original rock fabric along with small iron segregations in a clayey pallid horizon.
- (E) Dissolution of pisoliths giving rise to concentric opaque and clayey rings caused due to dismantling of ferricrete profile.
- (F) Vesicles filled by sparites : an indication of I st phase of calcretization.



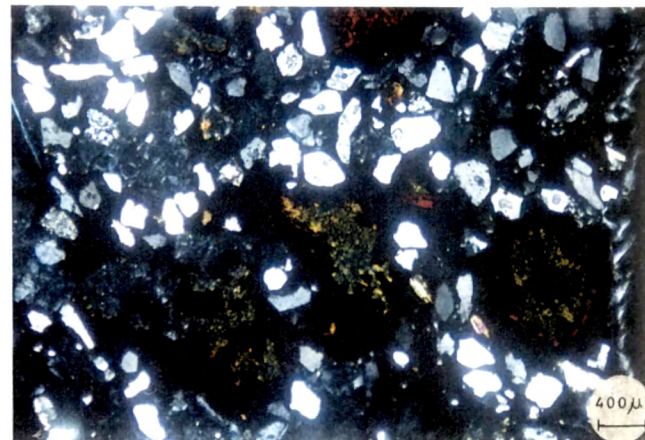
A



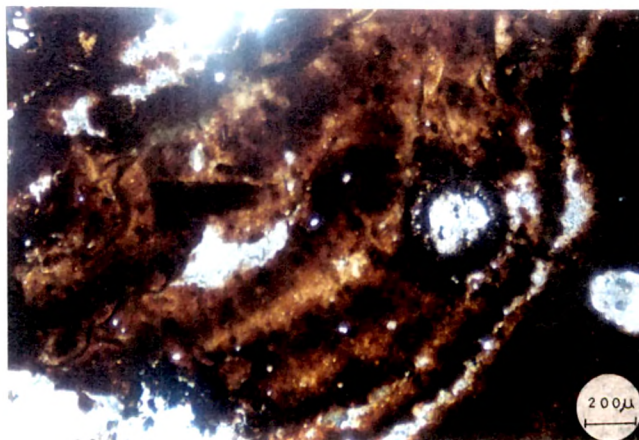
B



C



D



E

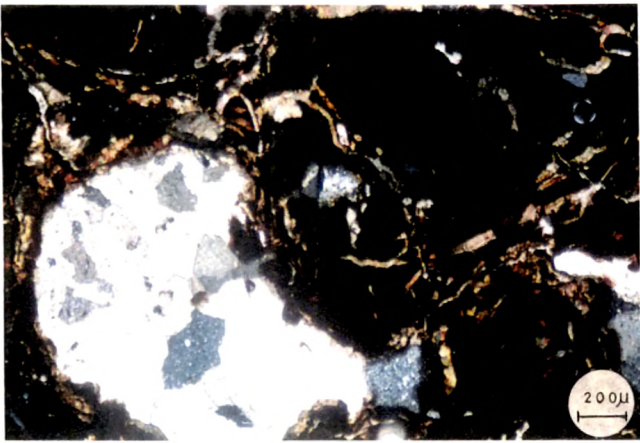


F

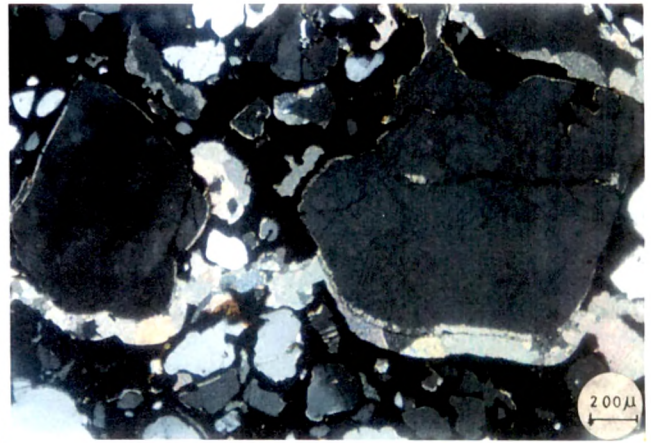
PLATE 5-6

Plate 5.7 Photo micrographs of ferricrete profiles elucidating

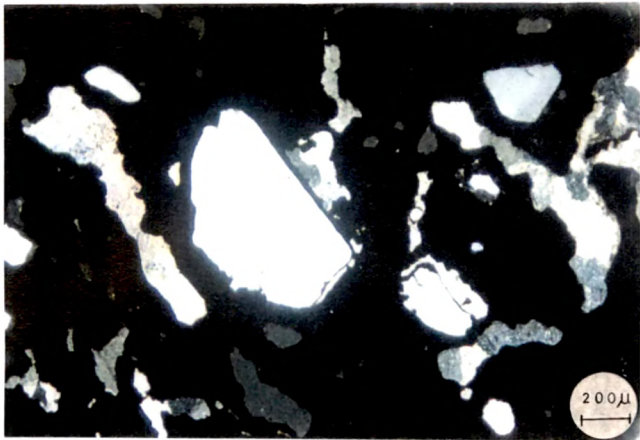
- (A) Sparitic fillings in the cavities of ferricretes denoting Ist phase of calcretization.
- (B) Sparites forming pendent cements around detritals.
- (C) Sparites filling the dissolution spaces around the corroded quartz skeletal grains.
- (D) Channel filled with sparites and development of micro laminations along channel wall due to calcite replacement.
- (E) Accumulation of cryptocrystalline silica along the fractures in mottled horizon, an indicator of microenvironmental changes within ferricrete profiles.
- (F) Micrites encompassing the ferricrete fragments, illustrative of II phase of calcretization.



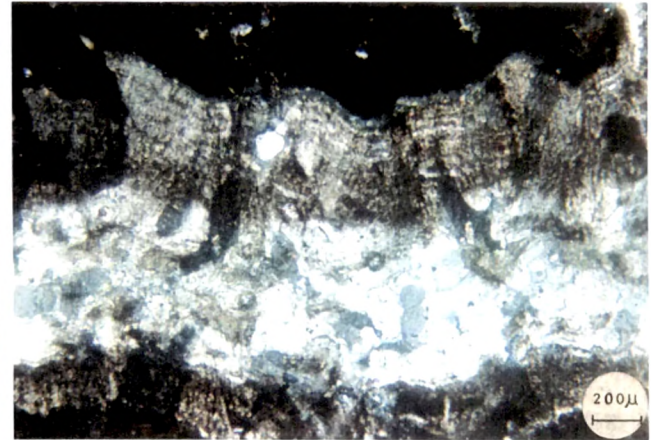
A



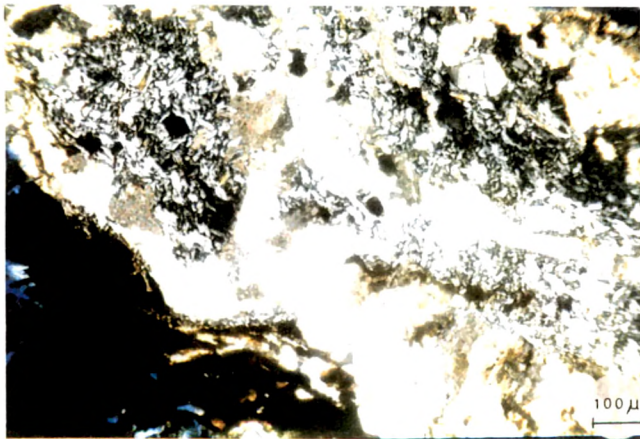
B



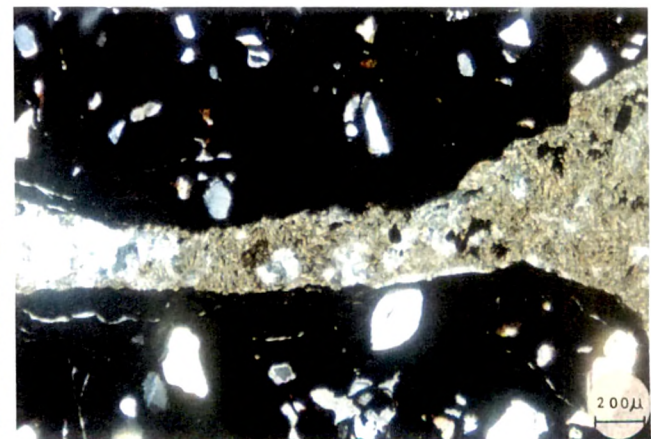
C



D



E

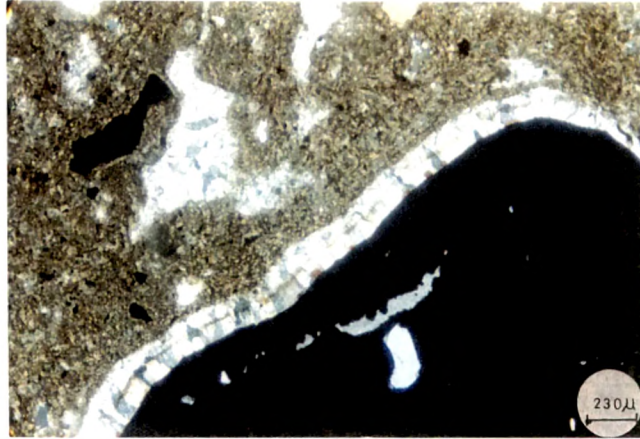


F

PLATE 5.7

Plate 5.8 · Photomicrographs of calcretized ferricretes depicting

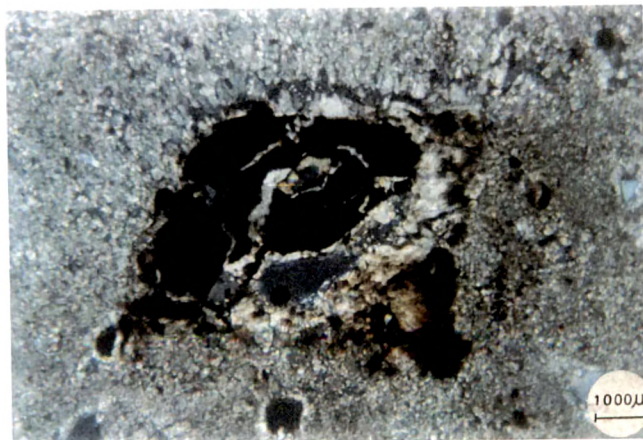
- (A) Neoformed sparites around ferricrete fragments developed from the II generation micrites - depicting maturity of calcretes.
- (B) Neoformed sparites around ferricrete fragments at an initial stage of calcite replacement.
- (C) Intense replacive action of calcites on ferricretes depicting the progression of calcretization.



A



B



C

PLATE 5-8

the precipitation of dissolved silica, leached from the upper horizons under changing physico chemical conditions.

The second phase of calcretization is evidenced by means of the presence of dusty micritic groundmass wherein the ferricretic nodules comprising the earlier phase of calcretization are enclosed (Plate 5.7 F). Formation of sparitic neocalcitans around the ferricrete nodules indicate the progression of calcretization at the cause of ferricretes (Plate 5.8 [A]). Ferricrete also exhibit progression of the calcite neoformation which in turn resulted in the formation of a calcrete layer wherein the relics of small ferricretic nodules or breccias are observed. Digestion of ferricrete nodules also begin along the boundaries of the ferricrete fragments (Plate 5.8 [B]). In the extreme stages of calcretization of ferricrete, ferricrete nodules are replaced by the calcite along fractures and boundaries (Plate 5.8 [C]).

CHEMISTRY AND MINERALOGY OF FERRICRETES

In order to understand the chemical kinetics during the ferricrete profile development, their dismantling, and subsequent phases of calcretization, the author has carried out geochemical (major oxides and trace elements) and mineralogical studies of the different horizons in the weathering profiles. Remarkable absence of a complete sequence of weathering profile (not even in a single location) coupled with dismantling of ferricrete profiles and contamination by calcretization has jeopardized the author, in applying the conventional techniques (McFarlane, 1987a,b; Esson, 1987; Balasubramaniam et al., 1987, Fitzpatrick and Schwertmann, 1982) helpful in understanding the weathering trends, neoformations, phases equilibria of different neoformed minerals etc. However, the author could not be able to correlate the geochemical data with the mineralogy to draw a possible scheme of weathering sequence and ferricretization.

Quantitative data on the major oxides and trace element concentrations of ferricrete, mottled and pallid horizons of the ferricrete profiles are provided in the Table 5.1. To understand the weathering trend and also to classify the ferricretes by adopting Schellman's (1981) classification, the author has plotted the ternary diagram, molar ratio

Sa. No.	Location	Dep (m)	LOI wt. %	SiO ₂ wt. %	Fe ₂ O ₃ wt. %	Al ₂ O ₃ wt. %	CaO wt. %	MgO wt. %	Zn ppm	Cu ppm	Mn ppm	Sr ppm	Ba ppm	B ppm
1	Ramgarh	0.3	5.7	47.0	13.0	23.9	11.0	4.7	50	22	63	247	27	2784
2		1.5	9.7	79.0	4.0	8.3	4.2	3.8	24	22	99	2786	239	3032
3		2.5	11.8	74.8	3.6	16.8	0.5	4.2	42	32	66	3618	151	809
4	Bandah	0.5	11.0	66.3	7.6	22.3	2.7	1.1	35	15	17	134	11	350
5		1.5	13.0	51.0	4.9	18.7	21.9	3.5	28	8	10	351	32	132
6	Chetral	2.5	17.0	52.1	10.8	24.4	9.5	3.2	83	17	61	1136	47	2115
7		3.7	7.0	89.4	0.5	9.1	0.5	0.5	4	7	6	120	22	3276
8	Savanta	1.0	7.8	72.6	8.7	16.6	0.8	1.0	97	17	1458	262	143	Ni
9		1.8	21.3	72.9	2.8	18.9	4.4	1.0	60	20	45	832	49	931
10		3.0	6.0	78.4	2.5	18.2	0.2	0.6	36	15	13	101	20	1985
11	Khenya	0.6	25.7	29.2	12.4	38.0	14.4	6.2	16	9	62	441	30	3067
12		2.5	12.7	61.8	5.8	9.9	11.3	11.2	15	9	28	656	25	312
13	Kaladongar	2.0	10.7	19.2	24.9	13.4	22.2	20.3	38	7	160	82	17	Ni
14		5.0	8.3	10.6	11.2	16.8	29.2	32.1	29	3	123	249	25	1762
15		10.0	12.1	55.1	4.8	18.9	2.2	19.0	25	15	35	98	23	929

Sa. No	Location	Depth (m)	SiO ₂ /Fe ₂ O ₃	SiO ₂ / Al ₂ O ₃	SiO ₂ / (Al ₂ O ₃ + Fe ₂ O ₃)	Fe ₂ O ₃ /Al ₂ O ₃	Ba/Sr
1	Ramgarh	0.3	7.15	1.9	0.8	0.26	0.07
2		1.5	39.3	9.1	4.16	0.23	0.11
3		2.5	41.1	4.2	2.4	0.10	0.03
4	Bandah	0.5	17.3	2.9	1.4	0.16	0.05
5		1.5	20.6	2.6	1.4	0.12	0.06
6	Chetral	2.5	9.5	2.0	1.0	0.21	0.02
7		3.7	355.5	9.4	6.0	0.02	0.11
8	Savanta	1.0	16.5	4.2	1.9	0.25	0.35
9		1.8	51.7	3.7	2.2	0.07	0.04
10		3.0	62.4	4.1	2.5	0.06	0.12
11	Khenya	0.6	4.7	0.7	0.4	0.15	0.04
12		2.5	21.2	6.0	2.6	0.28	0.03
13	Kaladongar	2.0	1.53	1.4	0.3	0.90	0.13
14		5.0	1.88	0.6	0.3	0.32	0.06
15		10.0	22.8	2.8	1.5	0.12	0.15

TABLE 5.1 MAJOR OXIDES AND TRACE ELEMENT CHEMISTRY OF FERRICRETE PROFILES

plots (Figure 5.3 A,B) of weathering profiles, by taking into account the silica, alumina and iron as bulk concentration.

Different oxide's molar ratio especially, silica / iron - indicative of desilicification, silica / aluminum, strontium / barium - indicative of hydrolysis and leaching, silica / sesquioxides - indicative of hydration, iron / alumina - indicative of oxidations are computed to understand geochemical processes during the development of ferricretes (Retallack, 1990)

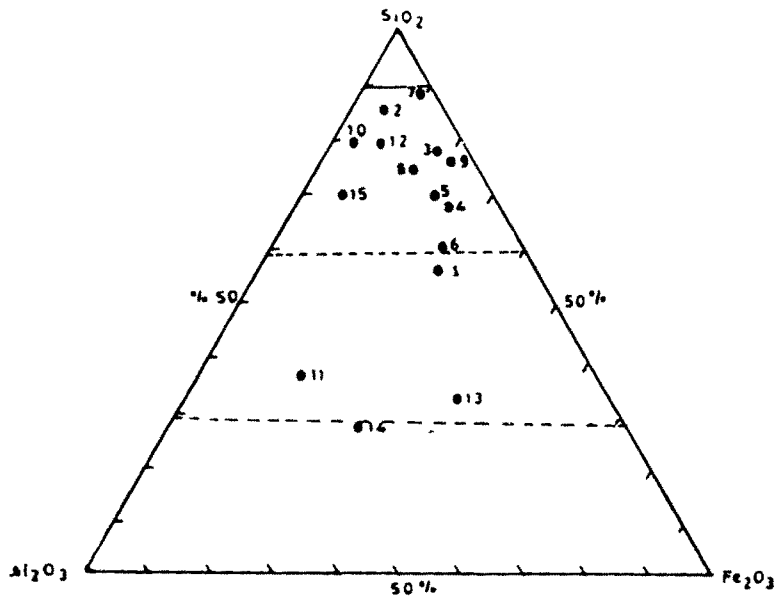
Among the trace elements Mn, Sr., Ba, B are incorporated to understand the micro - environmental conditions within the ferricrete profiles. The profile wise geochemical characteristics are briefly discussed as under

Ramgarh

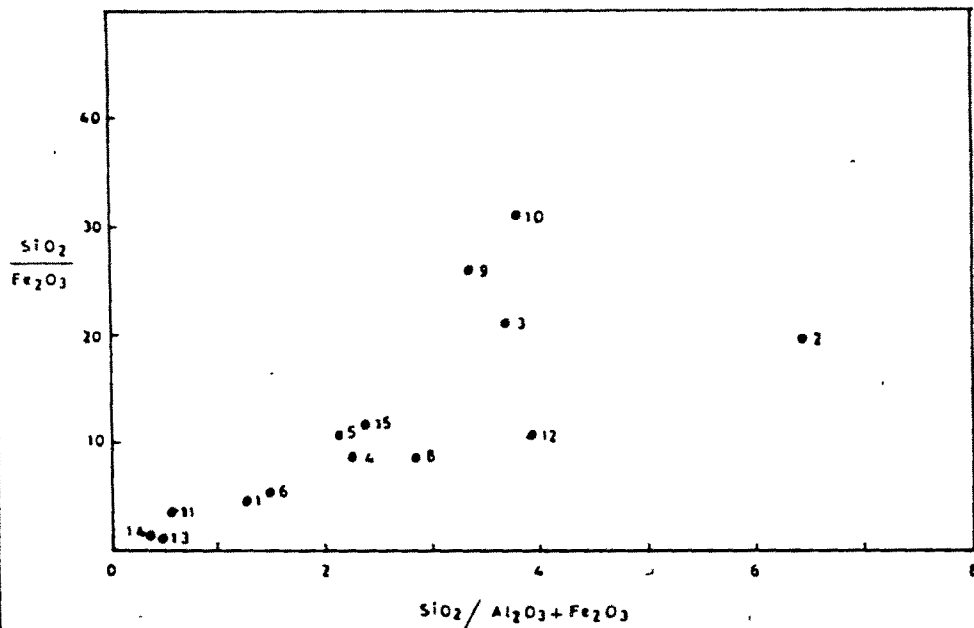
The top packed pisolithic horizon is characterized by higher alumina content (23.9 wt.%) among the sesquioxides. The silica content of this horizon is 47.0 % (Table 5.1, Figure 5.3 [A,B]). There is sudden spurt in the silica content in the underlying mottled horizon (79%) with a drop in iron (4%) and alumina content (8.3%). However, in the lower pallid horizon the alumina concentration enhances (16.8%) with a slight drop in the concentration of silica. Higher concentration of CaO and MgO in the pisolithic horizon over the lower horizons is due to the calcretization along fractures.

Desilicification in the upper horizon is evidenced by progressive decrease in silica / iron; silica / alumina values. The very low values of the Ba/Sr ratio again point to the retention of Sr in the profile, which is generally found in poorly leached weathering profiles. The iron / alumina ratio of the profile (0.26 - 0.10) indicate the spodic stage of the weathering profile. The progressive increase in the silica / sesquioxides ratio from the pisolithic to pallid horizon also point to the progressive increase in the concentration of hydrated minerals at the top.

Among the trace elements, the concentration of Mn, B, is relatively higher in the mottled horizon. While Zn shows depletion. This signifies the change in the pH conditions towards alkalinity in the mottled horizon.



(A) Ternary diagram of weathering trends



(B) Plots showing silica to sesqui-oxide ratios

Fig. 5.3 Geochemical trends in ferricrete profiles

Bandah

The upper brecciated ferricrete comprise silica, alumina and iron in the decreasing order of concentration. The underlying calcretized ferricretic horizon has higher concentration of CaO (21.9%), which can be better designated as calccrete. In spite of increase in the CaO and MgO concentration, the molar ratio of iron and sesquioxides remain almost similar to that of the overlying horizon.

Savanta

The salient geochemical characteristics of this profile are : reduction in the concentration of silica from pallid to pisolithic horizons, increase in iron and slight decrease in alumina content from pallid to pisolithic horizons, increase in calcium content at mottled horizon with slight decrease in silica and gradual decline in silica / iron (62.4 - 16.5%) from the pallid to pisolithic horizon indicating the relative enrichment of iron towards the top. Iron /alumina ratio of the profile is also characteristic of typical spodic horizon. Retention of strontium especially in higher concentration at the mottled and pallid horizons indicate poor leaching of the weathering profile (Rao and Krishnamoorthy, 1981; Retallack, 1991).

Khinya

The upper calcretized, brecciated ferricrete have alumina, silica, calcium, iron and magnesia in decreasing order of abundance. But, the underlying pallid horizon is characterized by higher content (twice that of ferricretes). In this horizon both calcium and magnesium concentration is also fairly higher than the ferricretes. Low molar strontium to barium ratio as well as higher concentration of strontium in both ferricretes and pallid horizons indicate the poor leaching conditions. Low molar ratio of silica / alumina (0.74) of ferricretes suggest the dominance of desilicification in the upper parts of the profile. This phenomenon is also supported by low silica / sesquioxides molar ratio suggesting an increase in hydrated oxyhydrates in the upper part.

Similar results i.e. desilicification and enhancement of oxyhydrates are evidenced in the ferricrete profile from Chetral area. The sudden spurt in the silica content in the mottled horizon is also akin to Savanta and Ramgarh ferricrete profiles.

Kaladongar

The salient geochemical characteristics of this profile show the concentration of iron at the top, particularly in sheeted ferricretes which is comparably higher (24.9 %) than other forms of ferricrete. The progressive increment of iron, and decrement of silica from the parent rock to the ferricrete clearly point that ferricretization is an enrichment process.

Silica / iron and silica / sesquioxides ratio of the profile again point to the desilicification and increase in the concentration of oxyhydrates in the upper parts of the profile. The Iron / alumina molar ratio of the sheeted ferricretes (0.90) is also characteristic of spodic horizons. The higher concentration of the strontium sandwiched between a lower concentration is however remains perplexing. The mobility of 'Mn' within the profile follows the trend of iron.

From these geochemical characteristics of the ferricrete profiles the following inferences can be made

1. Higher concentration of sesquioxides in the upper part of the weathering profiles is dominantly attributed to enrichment processes.
2. Desilicification is a dominant process operated in the upper parts of the ferricrete profiles.
3. The poor leaching of the pallid and mottled horizons as indicated by the higher concentration of Sr might have been responsible for the hike in the silica content (caused by precipitation of secondary silica that is generated from the upper horizons) in the upper parts of the mottled horizon.
4. The mobility of Mn within the ferricrete profiles (but for Ramgarh) follows the trend of iron.

- 5 Boron doesn't follow any definite trend within the ferricrete profile and hence their utility is not appreciated in deciphering the micro - environments.
- 6 The ferricretes predominantly fall within the kaolinized and weakly lateritised groups pointing that they are not well developed ferricretes.
- 7 Geochemical context wise, the ferricretes of the study area show close similarity to aluminous laterites.
- 8 Though calcretization has affected the bulk chemistry of the ferricrete profiles, the silica/iron, silica/alumina, silica/sesquioxide molar ratios remain the same, which is very well evidenced from the brecciated ferricretes and calcretized ferricrete of Bandah profile
- 9 The correlation analysis of the major oxide and trace element chemistry of the ferricrete profiles have revealed the negative correlation between silica and iron ($R = - 0.74$); silica and alumina ($R = - 0.40$). Among the trace elements negative correlation is evidenced with Zn - B; Mn - Sr, B. The negative correlation between the silica and sesquioxides can be interpreted in terms of desilicification and enrichment of alumina and iron. As the mobility of boron doesnot show any definite trend within the ferricrete profiles, the negative correlation of other trace elements with boron does not throw any significant light.
10. The chemical classification of the ferricretes indicate that ferricrete profiles of the study area are mostly in the in kaolinitic stage of weathering (Figure 5.3 A) to weakly lateritised groups (Schellman,1981).

MINERALOGY OF FERRICRETES

Since the microscopic techniques has not revealed much data on the mineralogical assemblages of the different horizon of the ferricrete profiles, samples of the representative horizons were subjected X - ray diffraction and the obtained results are presented in Tables 5.2 (A - J) and Figures 5.3 (A - J).

TABLE 5.2 A (Sa. No. 1)

Sr.No	2 - θ	d- spacing (A°)	I / I _o	Mineral (s)
1	21.29	4.17	20	Goethite
2	26.65	3.34	39	Quartz
3	29.42	3.034	100	Calcite
4	33.10	2.70	18	Goethite
5	35.63	2.518	17	Goethite
6	35.980	2.494	17	Calcite, Goethite
7	39.440	2.283	23	Quartz, Calcite
8	43.140	2.095	13	Calcite
9	47.63	1.908	13	Calcite
10	48.63	1.871	17	Calcite

TABLE 5.2 B (Sa. No 3)

Sr. No	2 - θ	d-spacing (A°)	I / I _o	Mineral (s)
1	20.910	4.245	30	Quartz
2	21.180	4.191	10	Goethite
3	21.400	4.149	11	Maghemite
4	26.650	3.342	100	Quartz
5	30.340	2.944	9	Maghemite
6	34.55	2.594	9	Goethite
7	36.510	2.459	13	Quartz
8	36.600	2.453	19	Goethite
9	39.450	2.282	9	Quartz
10	40.310	2.236	11	Quartz
11	41.060	2.196	8	Goethite
12	42.450	2.128	15	Quartz
13	50.140	1.818	17	Quartz
14	50.310	1.812	9	Maghemite
15	54.860	1.672	8	Quartz

TABLE 5.2 C (Sa. no. 4)

Sr.No	2 - θ	d - spacing (A°)	I / I _o	Mineral (s)
1	20.860	4.255	25	Quartz
2	21.290	4.17	25	Goethite
3	26.630	3.345	100	Quartz
4	29.400	3.036	16	Calcite
5	33.350	2.685	10	Goethite
6	36.570	2.455	10	Quartz
7	36.800	2.440	15	Goethite
8	36.900	2.43	13	Quartz, Goethite
9	39.480	2.281	12	Calcite
10	39.600	2.27	10	Quartz
11	53.430	1.713	9	Goethite

TABLE 5.2 D (Sa. no. 5)

Sr.No	2 - θ	d - spacing (A°)	I / I _o	Mineral (s)
1	12.200	7.249	3	Kaolinite
2	20.820	4.263	3	Quartz
3	23.030	3.859	6	Calcite
4	26.600	3.348	13	Quartz
5	29.400	3.036	100	Calcite
6	35.970	2.495	8	Calcite
7	36.570	2.455	2	Quartz
8	38.790	2.320	2	Kaolin
9	39.420	2.284	12	Quartz, Calcite
10	43.160	2.094	12	Calcite
11	47.160	1.926	4	Calcite
12	47.530	1.911	18	Calcite
13	48.510	1.875	12	Calcite
14	50.060	1.821	2	Quartz
15	56.580	1.625	2	Calcite
16	57.400	1.604	7	Calcite

TABLE 5.2 E (Sa. no. 6)

Sr. No.	2 - θ	d - spacing (A°)	I / I _o	Mineral (s)
1	20.930	4.241	21	Quartz
2	21.330	4.162	14	Goethite
3	24.180	3.678	15	Hematite
4	26.610	3.347	77	Quartz
5	29.430	3.033	100	Calcite
6	33.070	2.707	27	Goethite, Hematite
7	34.730	2.581	15	Goethite
8	35.580	2.521	18	Hematite
9	36.030	2.491	19	Goethite, Calcite
10	39.450	2.282	33	Quartz, Calcite
11	43.200	2.092	21	Calcite
12	47.570	1.910	24	Goethite, Calcite
13	48.530	1.874	21	Calcite
14	54.050	1.695	16	Hematite
15	57.450	1.603	17	Goethite, Calcite

TABLE 5.2 F (Sa. no. 8)

Sr.No	2 - θ	d - spacing (A°)	I / I _o	Mineral (s)
1	20.750	4.277	25	Quartz
2	26.580	3.351	100	Quartz
3	30.830	2.898	11	Magnetite
4	33.310	2.688	11	Goethite
5	36.530	2.458	11	Quartz
6	39.410	2.285	11	Quartz
7	50.130	1.815	24	Quartz

TABLE 5.2 G (Sa. no. 10)

Sr.No	2 - θ	d - spacing (Å)	I / I _o	Mineral (s)
1	12.330	7.173	25	Kaolinite
2	17.740	4.996	7	Goethite, Maghemite
3	19.730	4.496	4	Maghemite, Kaolinite
4	20.810	4.265	24	Quartz
5	21.190	4.189	3	Goethite
6	24.840	3.582	8	Kaolinite, Maghemite
7	26.600	3.348	100	Quartz
8	29.800	2.996	3	Maghemite
9	34.920	2.567	3	Goethite, Kaolinite
10	35.990	2.493	3	Goethite
11	36.500	2.460	9	Quartz
12	38.360	2.345	3	Kaolinite
13	39.440	2.283	7	Quartz
14	40.230	2.240	4	Quartz
15	42.390	2.131	6	Quartz
16	42.480	2.126	5	Quartz
17	45.140	1.996	6	Goethite
18	45.730	1.982	6	Quartz
19	50.090	1.820	15	Quartz
20	54.810	1.674	4	Quartz

TABLE 5.2 H (Sa. no. 11)

Sr. No.	2 - θ	d - spacing (Å)	I / I _o	Mineral (s)
1	21.320	4.174	19	Goethite
2	23.100	3.847	14	Calcite
3	26.600	3.348	20	Quartz
4	29.450	3.031	100	Calcite
5	36.060	2.489	22	Calcite
6	36.900	2.434	12	Goethite, Maghemite
7	39.480	2.281	23	Calcite
8	43.250	2.090	23	Calcite
9	47.740	1.904	13	Calcite
10	48.600	1.872	17	Calcite
11	57.480	1.602	15	Goethite

TABLE 5.2 .I (Sa. no 12)

Sr. No	2 - θ	d - spacing (A°)	I / I _o	Mineral (s)
1	22.850	3.889	12	Calcite
2	26.420	3.371	19	Goethite
3	29.250	3.051	100	Calcite
4	30.460	2.932	19	Magnetite
5	30.580	2.921	17	Goethite
6	35.780	2.508	19	Calcite
7	36.620	2.452	8	Quartz
8	36.780	2.442	9	Goethite,Magnetite
9	39.310	2.290	23	Calcite
10	43.030	2.100	18	Calcite
11	46.940	1.934	8	Goethite
12	47.060	1.929	9	Calcite
13	47.350	1.918	16	Calcite
14	48.410	1.879	19	Calcite
15	57.350	1.605	10	Goethite
16	57.510	1.601	9	Manganesoferrite (?)

TABLE 5.2. J (Sa. no. 13)

Sr.No.	2 - θ	d - spacing (A°)	I / I _o	Mineral (s)
1	21.240	4.180	100	Goethite
2	23.600	3.767	30	Maghemite
3	25.510	3.489	30	Maghemite
4	26.670	3.340	78	Quartz
5	29.490	3.027	44	Calcite
6	33.280	2.690	61	Goethite
7	34.990	2.562	36	Magnetite
8	36.010	2.492	38	Calcite
9	36.720	2.446	85	Goethite,Quartz
10	39.600	2.274	31	Quartz,calcite
11	41.250	2.187	39	Goethite
12	49.290	1.847	33	Quartz
13	50.880	1.793	35	Goethite
14	53.280	1.718	48	Maghemite

TABLES 5.2 (A - J) XRD DATA OF FERRICRETE PROFILES

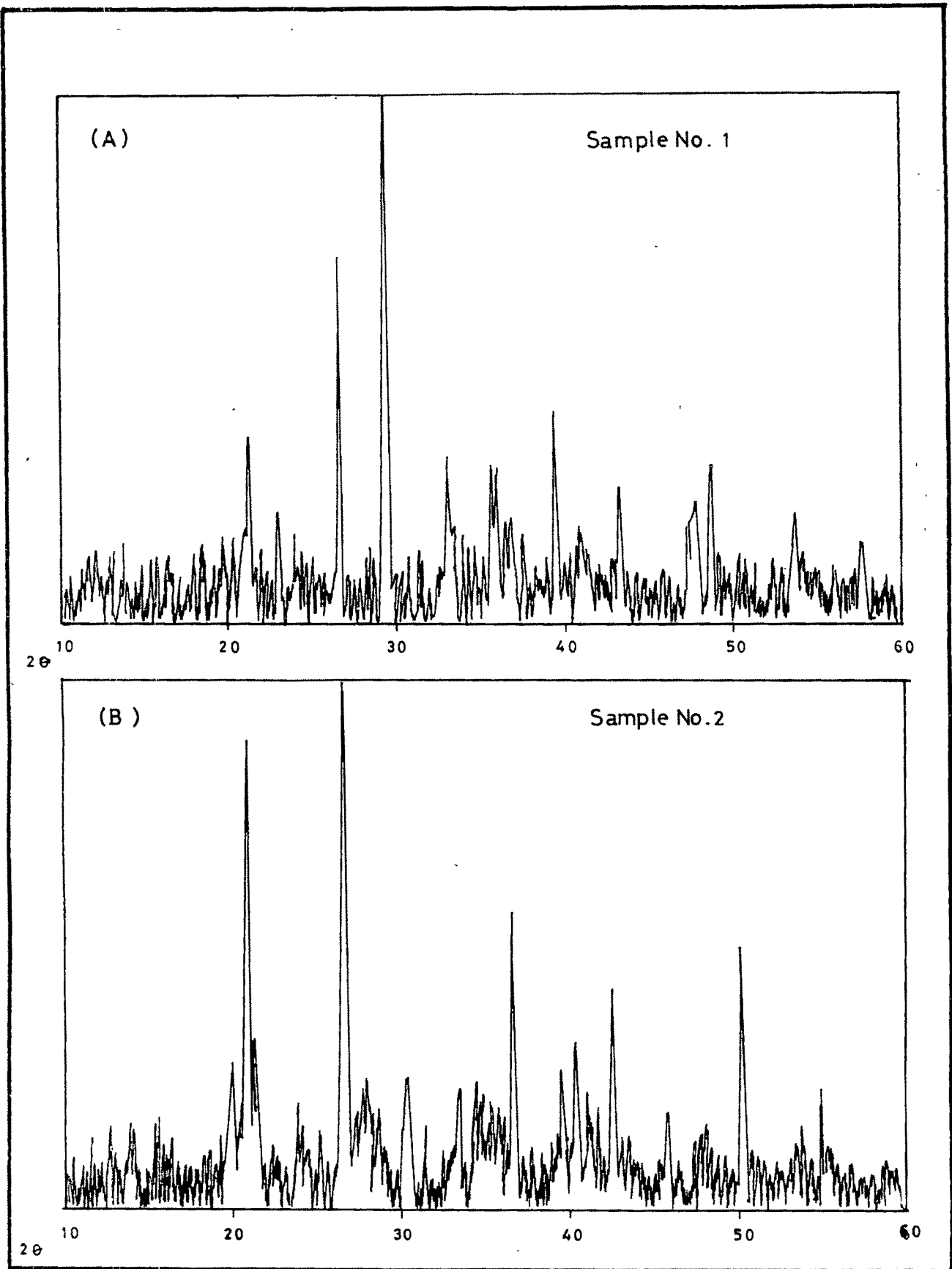


Fig. 5.2 X-ray Diffractogram of ferricrete profiles

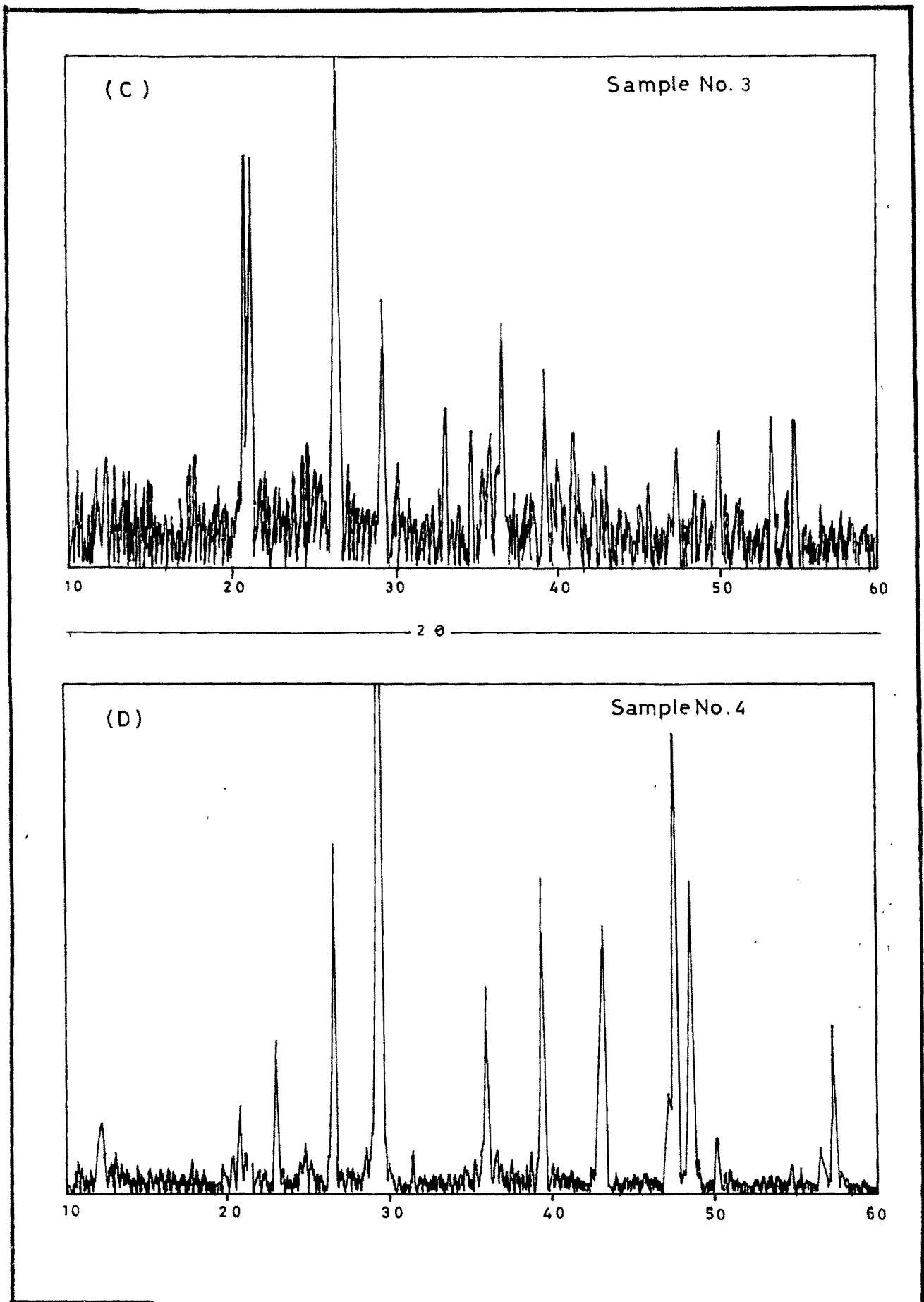


Fig. 5.2 X-ray Diffractogram of ferricrete profiles

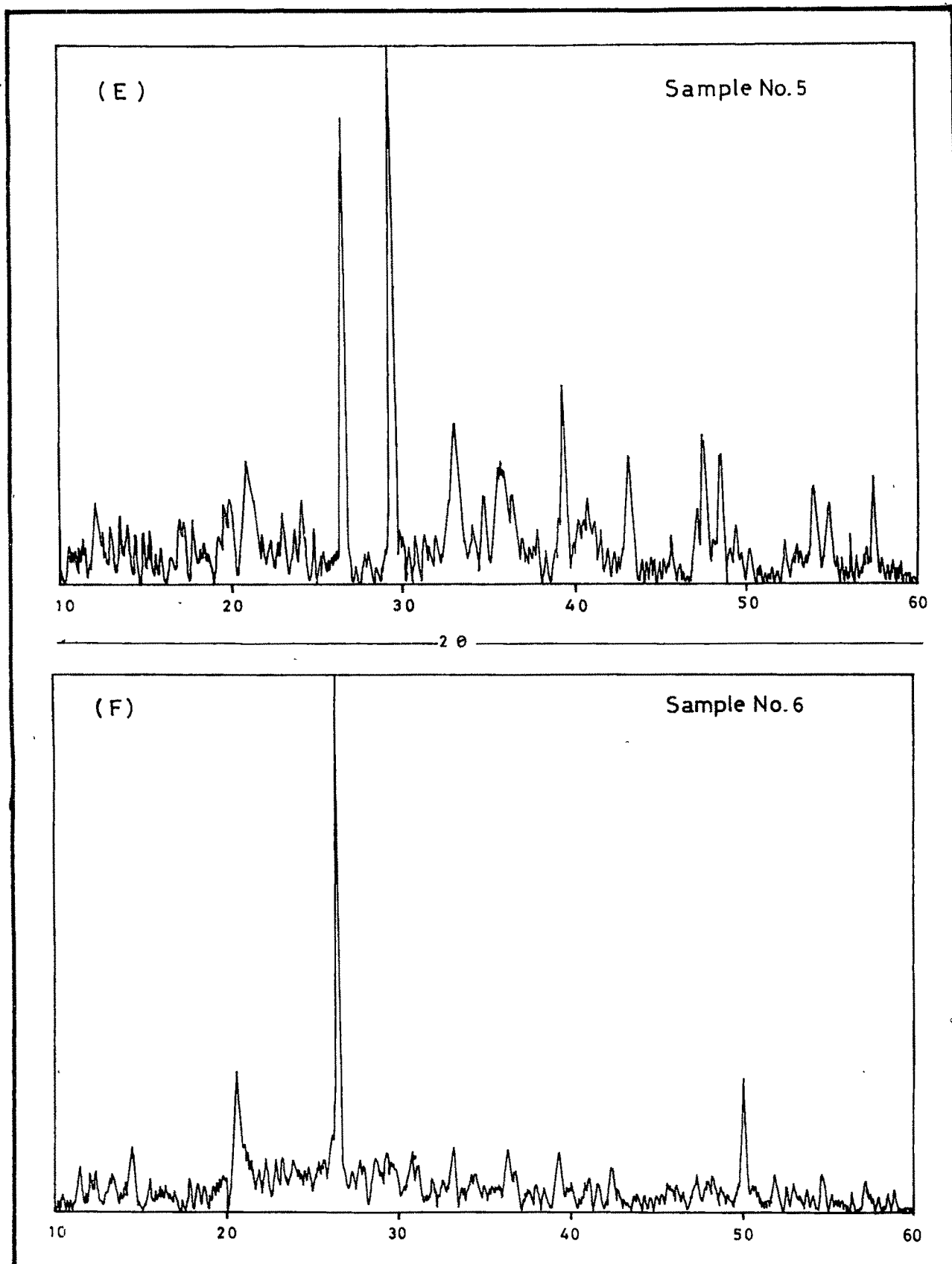


Fig. 5.2 X-ray Diffractogram of ferricrete profiles

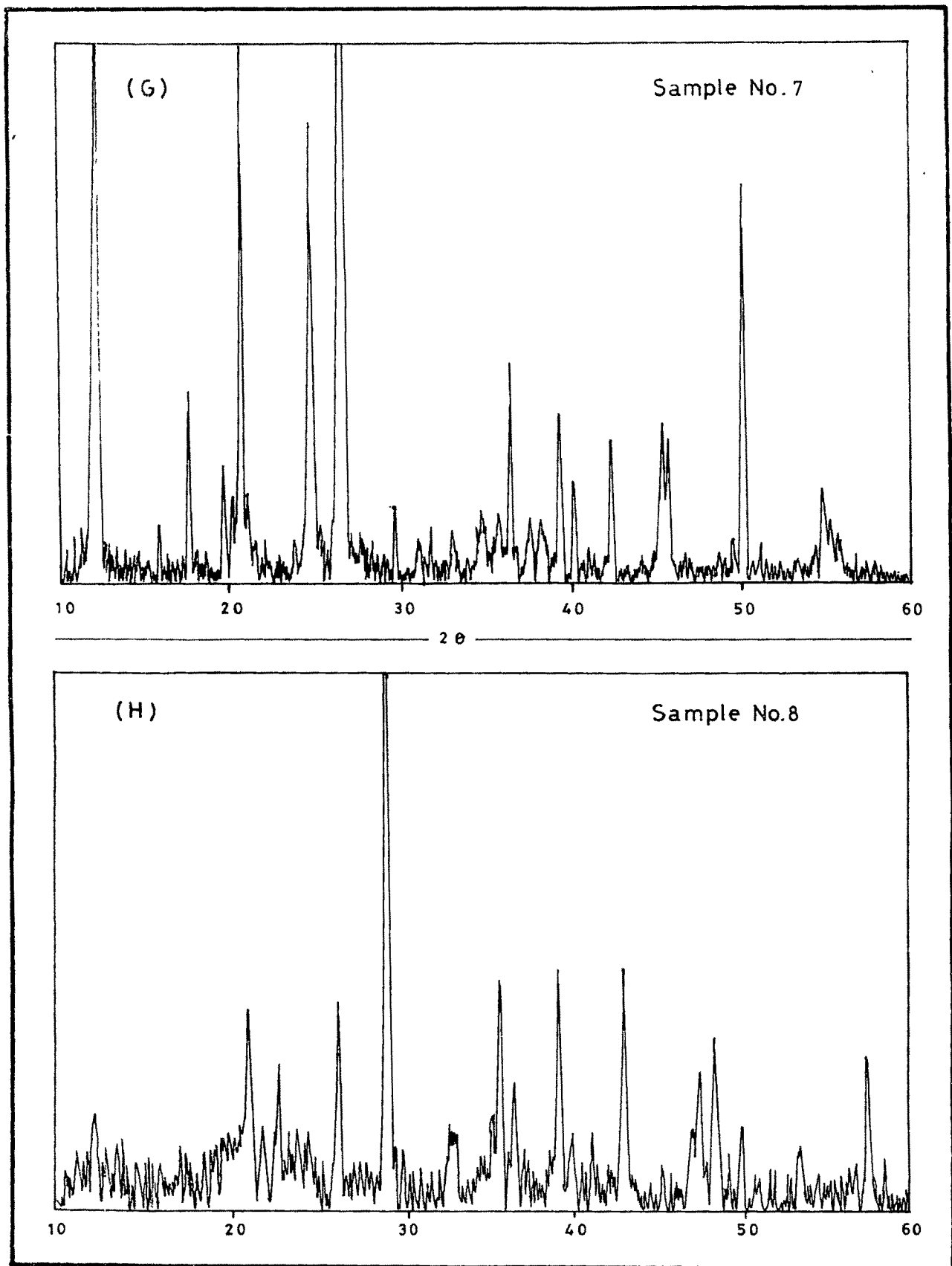


Fig. 5.2 X - ray Diffractogram of ferricrete profiles

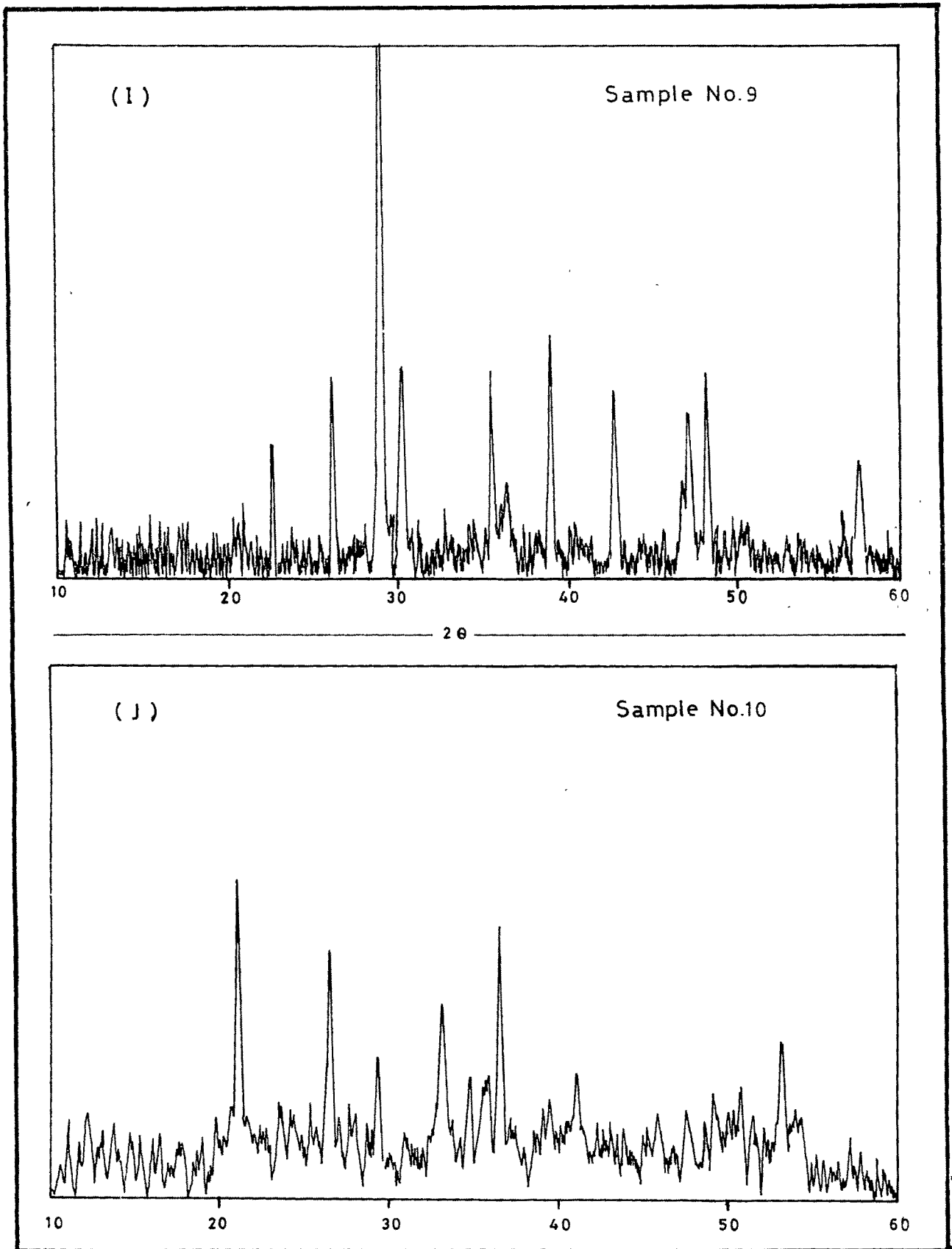


Fig. 5.2 X-ray Diffractogram of ferricrete profiles

Bardossy (1979a) recognized near about 170 minerals in the lateritic weathering profiles. The mineral assemblages of ferricretic profiles from study area comprise goethite, hematite, maghemite among the iron bearing minerals, kaolin, smectite (montmorillonite) among the aluminosilicates and quartz.

The iron bearing minerals of the hard ferricretic cappings are predominantly goethitic with occasional hematite (Chetral), magnetite (Savanta and Kaladongar) and maghemite (Savanta and Kaladongar). The other abundant mineral is quartz. Wherever the ferricretes underwent calcitization the concentration of calcite becomes prominent.

The mottled zones and pallid zone mostly comprise kaolin, quartz with subordinate quantities of goethite and maghemite. Presence of montmorillonite in the Khinya profile is rather an exception. The formation of montmorillonite instead of kaolin can be attributed to the higher concentration of 'Mg' and 'Ca' from the underlying parent rock i.e. Nummilitic limestone.

DISCUSSION

The ferricretic duricrusts form the most conspicuous residual deposit of the arid terrains of the Thar desert. These weathered mantle which are associated with varied parental rocks, belonging to different age groups (Jurassic - Tertiary) display heterogeneity in their development. From the foregoing account on their field distribution pattern, degree of maturity in terms of development of various horizons, geochemical and mineralogical parameters, the author has attempted to understand and established various correlations, mechanism and the micro-environmental changes leading to its genesis. In all the profiles studied so far, a clear saprolitic zone couldn't be traced and hence pallid zone need to be recognized as a separate unit. Kaolinisation of feldspars is the most significant feature observed in this zone. The textural features of the parent rocks (sandstone / limestones) are not completely obliterated. Slight corrosion of the detrital quartz also shows sign of separation by clay and sesquioxides. Some important minerals of this zone are kaolin and

quartz with occasional goethite. The chemistry of this zone is also in conformation to the mineralogy by way of high silica and alumina content.

The mottled zone, which has been considered as a part of the pallid horizon also needs to be considered as a separate unit, this is on account of dismantling of the profile and contamination (by calcretization) commonly seen upto the depth of mottled zone. The mineralogy of this zone is again akin to the pallid zone showing the predominance of kaolin and quartz. However, significant increase in the percentage of goethite indicates the enrichment of iron than that of pallid zone. The small scale migration of iron in this zone has been ascribed to the concentration of iron compounds, which in turn form fine to larger nodules that ultimately result in the generation of mottles (Nahon, 1987). McFarlane (1983a) proposed the segregation of iron to form pisoliths in the upper parts of the profile due to pedoturbations. But, the fact remains that the iron accumulation in the weathering profile is not exclusively due to enrichment phenomena. The most conspicuous feature that the author has observed in this zone, is the sudden spurt in the silica content comparing to the adjoining zones. Micromorphological evidence (presence of secondary silica along fractures and cavities - Plate 5.7 E) also supports the chemical data. The presence of silica in lower mottled zone indicates the change in physico-chemical environment. Wherein, the low pH acidic environment in upper ferricretic horizon leads to desilicification and forms silica gel. This gel on percolation to the lower mottled horizon gets precipitated as cryptocrystalline silica.

This phenomenon of silica precipitation is attributable to the change in pH conditions from neutral to near alkaline conditions (Balasubramaniam et al., 1981; Morris and Fletcher, 1987; Koln, 1992). The poor leaching conditions of the mottled zone (as evidenced by the Ba/Sr molar ratios) might have been responsible for the elevation of pH.

Also, the ubiquitously persistent upper most duricrust horizon is characterized by the mineral assemblages of goethite and quartz. Occasionally hematite (Chetral) and maghemite are also encountered (Savanta and Kaladongar). From the chemistry it is evident that the upper most horizon is rich in alumina than that of iron. This points to the

fact that the goethite in the ferricrete is predominantly Alumina rich (Schwertmann and Taylor, 1977, Fitzpatrick and Schwertmann, 1982) The prevalence of Al availability during goethite formation is attributed to a low pH and the presence of clay minerals especially kaolin (Fitzpatrick and Schwertmann, 1982).

The presence of Al rich goethite is good indicator of desilicification in acidic conditions (Schwertmann and Taylor, 1977) This observation as proposed by the author by way of silica / alumina; silica / iron and silica /sesquioxide molar ratios, are also strongly supported by the micromorphological evidence i.e. dissolution of quartz in the ferricretes (Plate 5.6 A) This process of disappearance of kaolin, corrosion and dissolution of quartz, formation of Al-goethite are the strongest evidences of development of the ferricretes under a typical lateritic weathering conditions (Little and Gilkes, 1982, Didier et al , 1983)

The subsequent dismantling of ferricrete profile is evidenced from the dismantling of pisoliths (Plate 5 6 E), and dissolution along the fractures (Nahon, 1987).

Superimposition of calcretization on the dismantled ferricrete has evidently taken place in two phases. The earlier phase of calcretization is marked by the coarse, clear sparites occupying the fractures, vesicles (Plates 5 6 F, 5.7 A); as pendent cements around detritals (Plate 5 7 A) and channel fillings (Plate 5.7 D). The microlaminations along the channel walls can be either due to replacement or by successive phases of coating. The second phase of calcretization is represented by drusy micritic groundmass encompassing the fragmented ferricrete fragments (Plate 5 7 F) Neof ormation of sparites along the ferricrete fragments and replacive reaction (Figure 5 8 A - C) gives strong indications of the change in the weathering processes i.e. from lateritic to calcretic, which must have been triggered by climatic changes.

GENESIS OF FERRICRETES

It is evident from the foregoing account that the ferricretes are the product of lateritic weathering that have been subjected to dismantling and later phases of calcretization. Accordingly, the author has recognized in all six stages (Figure 5 4) through which an overall evolution of ferricrete profiles have taken place. These evolutionary stages are

- Stage 1 This stage is marked by the generation of saprolite horizon over the ferruginous sandstones and limestones
- Stage 2 Further downward movement of weathering front, resulted in the development of a kaolinitic pallid zone from the previously available saprolite horizon
- Stage 3 Downward progression of weathering front and the generation of a mottled zone with a relatively small spaced pisolithic variety of ferricretes
- Stage 4 Continuous enrichment of iron, by the process of desilicification and formation of Al rich goethites, controlled migration of iron and the generation of packed pisolites. Development of sheeted type ferricretes due to high rate of sesquioxide cementing
- Stage 5 Dismantling of ferricretes due to the predominance of erosional processes over residual process. Development of fractures and brecciation of ferricretes, and infilling of the sparites (**first phase of calcretization**)
- Stage 6 Fragmentation of the ferricretes followed by the **second phase of calcretization** (progressive maturity of the calcretization is evidenced from the digestion of ferricrete fragments by calcite).

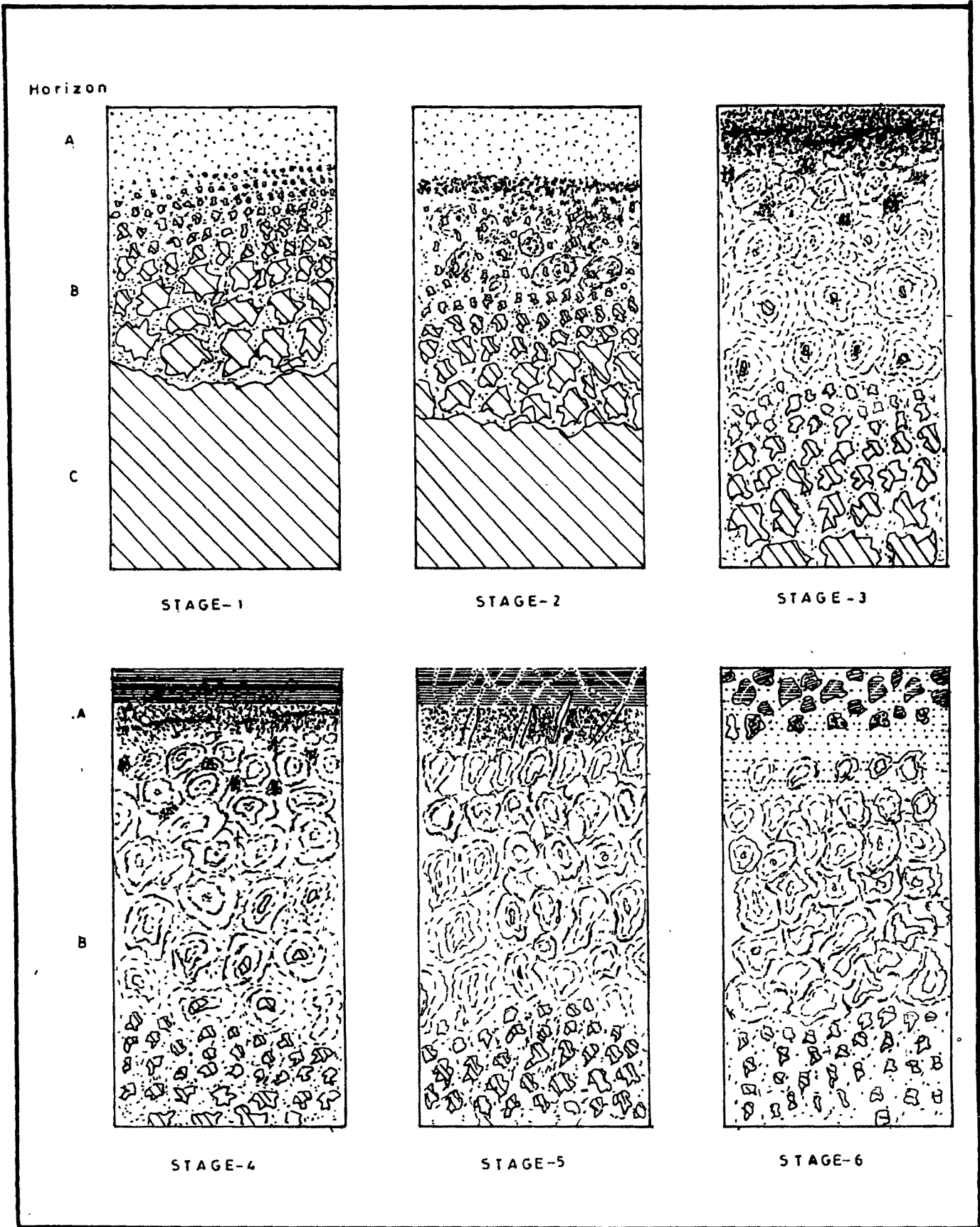


Fig. 5.4 Developmental stages of ferricretes

The above discussion leads to the following conclusions

- 1 The ferricretes of the study area are the product of lateritic weathering and mostly in kaolinitic stage of weathering
- 2 The lateritic weathering might have been of Neogene period characterized by a relatively humid and warm environment
- 3 The duricrust cappings are mostly rich in Al - goethite than in iron oxides and oxyhydrates.
- 4 The dismantling of ferricrete profiles and subsequent deposition of Shumar Formation (comprising ferricrete clasts) indicate that a wetter phase with dominance of erosion followed by the residual accumulation, probably during late Neogene - early Pleistocene period
- 5 The onset of aridity during middle Pleistocene was responsible for the varied phases of calcretization in ferricretes